ORIGINAL ARTICLE

ORAL DISEASES 🐾 WILEY

A novel *ENAM* mutation causes hypoplastic amelogenesis imperfecta

Shunlan Yu | **Chenying Zhang** | **Ce Zhu** | **Junkang Quan** | **Dandan Liu** | **Xiaozhe Wang** | **Shuguo Zheng**

Department of Preventive Dentistry, National Clinical Research Center for Oral Diseases, National Engineering Laboratory for Digital and Material Technology of Stomatology, Beijing Key Laboratory of Digital Stomatology, Peking University School and Hospital of Stomatology, Beijing, China

Correspondence

Shuguo Zheng and Xiaozhe Wang, Department of Preventive Dentistry, National Clinical Research Center for Oral Diseases, National Engineering Laboratory for Digital and Material Technology of Stomatology, Beijing Key Laboratory of Digital Stomatology, Peking University School and Hospital of Stomatology, 22 Zhongguancun South Avenue, Haidian District, Beijing 100081, China.
Email: kqzsg86@bjmu.edu.cn; neptunewxz@163.com

Funding information

Peking University School and Hospital of Stomatology Science Foundation for Young Scientists, Grant/Award Number: PKUSS 20170106 and PKUSS20180103

Abstract

Objectives: To identify the genetic cause of one Chinese family with hypoplastic amelogenesis imperfecta (AI) and explore the relationship between genotype and its phenotype.

Material and Methods: One Chinese family with generalized hypoplastic AI was recruited. One deciduous tooth from the proband was subjected to scanning electron microscopy. Whole-exome sequencing was performed and identified mutation was confirmed by Sanger sequencing. Bioinformatics studies were further conducted to analyze potential deleterious effects of the mutation.

Results: The proband presented a typical hypoplastic AI phenotype whose teeth in deciduous and permanent dentitions showed thin, yellow, and hard enamel surface. The affected enamel in deciduous tooth showed irregular, broken, and collapsing enamel rods with borders of the enamel prisms undulated and structural shapes of prisms irregular. A novel homozygous nonsense mutation in the last exon of the enamelin *(ENAM)* gene (NM_031889.3; c.2078C>G) was identified in the proband, which was predicted to produce a highly truncated protein (NP_114095.2; p.(Ser693*)). This mutation was also identified in the proband's parents in heterozygous form. Surprisingly, the clinical phenotype of the heterozygous parents varied from a lack of penetrance to mild enamel defects. Additional bioinformatics studies demonstrated that the detected mutation could change the 3D structure of the ENAM protein and severely damaged the function of ENAM.

Conclusion: The novel homozygous *ENAM* mutation resulted in hypoplastic AI in the present study. Our results provide new genetic evidence that mutations involved in *ENAM* contribute to hypoplastic AI.

KEYWORDS

amelogenesis imperfecta, *ENAM*, hypoplastic, mutation

1 | INTRODUCTION

Enamel is a mineralized tissue consisting of hydroxyapatite crystals and largely generated by ameloblasts. The composition and morphology of the mineral components within the enamel play essential roles in the physical properties and physiological function of the tissue. The unique molecular and cellular activities have been underway during amelogenesis, which was reflected by enamel's

---

final composition (Paine et al., 2001). Many genes were proved to be associated with the process of amelogenesis and mutations in them were known to cause amelogenesis imperfecta (AI), such as genes encoding the enamel matrix proteins (*AMELX*, *AMBN*, and *ENAM*) and the enamel proteinases (*MMP20* and *KLK4*), other genes encoding proteins that mediate or affect cell adhesion (*LAMA3*, *LAMB3*, *COL17A1*, *FAM83H*, and *ITGB6*) or were thought to be involved in endocytosis, calcium transport and pH sensing (*WDR72*, *SLC24A4*, and *GPR68*, respectively), and master controllers of amelogenesis (*FAM20A and DLX3*) had also been implicated. In addition, mutations in genes encoding proteins for which their function in amelogenesis was less clear (e.g., *ODAPH*, *AMTN*, *ACP4*, *RELT*, and *SP6*) were also known to cause AI (Gadhia et al., 2012; Kim et al., 2019; Seymen et al., 2016; Smith et al., 2017, 2020). More knowledge about these genetic influences on the process of amelogenesis leads to better understanding of the biological mechanism of enamel formation. Deviations from normal genetic programming during development may result in AI.

AI is a genetic disease affecting the structure, composition, and quantity of tooth enamel. The prevalence of AI has been reported to be 1 in 700 among an isolated Swedish population (Bäckman & Holm, 1986) and around 1 in 14,000 among the US population (Witkop, 1988). Many different inheritance patterns are existed in AI, including autosomal dominant, autosomal recessive, X-linked dominant, or X-linked recessive heredity (Witkop, 1988).

As a heterogeneous group of genetic conditions characterized by defective enamel, AI can be broadly classified based on the enamel phenotype, although mixed phenotypes frequently exist. Defects during the secretory stage tend to cause hypoplastic AI, for which the enamel is absent or thin and variably mineralized. Defects during the maturation stage generally result in hypomineralized AI, where the enamel is of full-thickness but is weak and fails prematurely. Hypomineralized AI can be further subdivided into hypomaturation and hypocalcified AI that produce brittle and soft enamel, respectively (Smith et al., 2017). AI may present as an isolated phenotype or may be associated with a syndrome.

AI enamel is abnormally thin, soft, fragile, pitted, and/or discolored, causing patients severe embarrassment, eating difficulties and pain. Clinically, the enamel in the hypoplastic type exhibits hard and translucent with reduced thickness (volume). Usually, it may be localized as pits or horizontal ridges or can be generalized with the entire enamel thickness being markedly reduced. Hypoplastic AI could be caused by mutations in *AMELX* (Lagerström et al., 1991), *ENAM* (Rajpar et al., 2001), *AMBN* (Poulter, Murillo, et al., 2014), *ACP4* (Seymen et al., 2016), *LAMA3* (Yuen et al., 2012), *LAMB3* (Poulter, El-Sayed, et al., 2014), and *COL17A1* (McGrath et al., 1996).

In this study, the phenotypic characteristics and detailed ultrastructure of the enamel in one novel autosomal-recessive mutation in *ENAM* gene (c.2078C>G, p.(Ser693*)) were reported. In this family, the affected proband with homozygous *ENAM* mutation showed generalized hypoplastic enamel with almost no enamel covering dentin. The clinical phenotype of the parents with heterozygous *ENAM* mutation varied from a lack of penetrance to mild enamel defects.

2 | MATERIALS AND METHODS

2.1 | Subjects

This study was ethically approved by the Ethical Committee of Peking University School and Hospital of Stomatology (issue number: PKUSSIRB-201631124) and was conducted following the Declaration of Helsinki principles. All participants or their guardians signed written-informed consent.

The proband was an 8-year-old girl with no health concerns or allergies. Her parents complained that the girl's erupted teeth were esthetically impaired. As the results of clinical and radiologic examinations confirmed to the clinical diagnostic criterion of hypoplastic AI (Witkop, 1988), diagnosis was made accordingly. Detailed clinical and radiologic examinations were also performed for the proband's family members.

Totally six healthy controls with age- and gender-matched with the proband were included, three for genotype analysis and three for phenotype analysis.

2.2 | Scanning electron microscopy

One exfoliated deciduous molar from the proband was collected and one deciduous molar from a normal individual of similar age was used as control. All extracted teeth were rinsed with 0.1 M phosphate buffer (pH 7.2) and were sectioned longitudinally in the buccolingual direction using a peripheral diamond. The cut sides were polished first, acid-etched for exactly 15 s with 40% phosphoric acid to remove the smear layer, dehydrated with 70% alcohol, dried in air.

Each section from the selected teeth was sputter-coated with gold and mounted on an aluminum stub for examination by scanning electron microscopy (SEM) (SU8010, Hitachi). Images were obtained at magnifications between 1000× and 2000×.

2.3 | DNA collection

Peripheral blood samples were collected from the participants and genomic DNA was extracted using TIANamp Blood DNA mini kit (Tiangen) following the manufacturer's instruction.

2.4 | Whole-exome sequencing and data analysis

Three micrograms of the patient's genomic DNA were prepared for whole-exome sequencing (WES) with the Agilent SureSelect

XT Library Prep Kit according to the manufacturer's protocol (Agilent Technologies). Sequencing was performed using a 100-bp paired-end protocol on an Illumina HiSeq2500 (Illumina). Agilent SureSelect Human All Exon V5 Enrichment System (Agilent Technologies) was used as the capture reagent. The sequencing reads were aligned to the human reference genome (GRCh37) using the Burrows-Wheeler aligner (Li & Durbin, 2009). With a series of bioinformatics tools, such as Samtools, Genome Analysis Tool Kit, and Annovar (Hintzsche et al., 2016), the sequence variants were annotated with dbSNP build 150 and filtered with a cut-off value of 0.01 for the minor allele frequency. Exome depth was used for CNV analysis according to the developer's guidelines (Plagnol et al., 2012).

Available genomic databases (Exome Variant Server, Genome aggregation database, and a local Paris Descartes Bioinformatics platform database) were used to filter variants in exon-intron boundaries, exonic and splicing variants, and exclude variants with a frequency >1%. Variants with a Combined Annotation Dependent Depletion (CADD; version 1.3) score ≥15 were prioritized, and those in genes already known to cause AI were highlighted for segregation analysis, including *AMELX*, *ENAM*, *AMBN*, *MMP20*, *KLK4*, *ITGB6*, *LAMB3*, *LAMA3*, *COL17A1*, *AMTN*, *FAM83H*, *WDR72*, *SLC24A4*, *FAM20A*, *DLX3*, *C4orf26*, *GPR68*, *ACPT*, *ACP4*, *ODAPH*, *RELT*, and *SP4* (Gadhia et al., 2012; Kim et al., 2019; Seymen et al., 2016; Smith et al., 2017, 2020).

2.5 | PCR amplification and Sanger sequencing

An *ENAM* mutation identified by WES was confirmed by Sanger sequencing. The exons and exon–intron boundaries of the *ENAM* gene were amplified by polymerase chain reaction (PCR) using the intron–exon specific primers (table S1) as described previously (Chan et al., 2010). DNA polymerase was purchased from Takara Technologies. In brief, the PCR reactions were carried out in a DNA Engine PTC-200 using the program described elsewhere (Zhang et al., 2017). The amplification products were bidirectionally sequenced using an ABI 3,730 XL automatic sequencer (Applied Biosystems, Foster City, CA). DNA sequences were analyzed using NCBI databases and the BLASTN (BLAST nucleotide) program (http://blast.ncbi.nlm.nih.gov/).

2.6 | Prediction of damaging effects

Sequential data processing using CADD (Kircher et al., 2014) (Combined Annotation Dependent Depletion, http://cadd.gs.washington.edu/) and M-CAP (Jagadeesh et al., 2016) (Mendelian Clinically Applicable Pathogenicity, http://bejerano.stanford.edu/MCAP) were performed to predict deleteriousness of the detected mutation. Additionally, the online program Mutation Taster (Schwarz et al., 2014) (http://www.mutationtaster.org) was also used to predict if the mutation was disease-causing. To analyze the effect of the

mutation on the molecular structure of ENAM protein, the three-dimensional (3D) structures of wide-type and mutant *ENAM* were predicted in silico using I-TASSER (Yang & Zhang, 2015) (Iterative Threading Assembly Refinement, https://zhanglab.ccmb.med.umich.edu/I-TASSER/).

3 | RESULTS

3.1 | Clinical findings

The proband was an 8-year-old girl presenting a typical hypoplastic AI phenotype from a non-consanguineous family. Her pedigree contained nine family members without similar manifestation (Figure 1a), which indicated an autosomal-recessive inheritance pattern. The enamel of the permanent teeth, including first molars and the recently erupted mandible and maxillary incisors of the proband was thin, yellow, and with hard texture (Figure 1b–e). The characteristics of enamel were more remarkable in the images of amplification of mandible and maxillary incisors, although there was some pigmentation in the lingual side of maxillary incisors (Figure 1d and e). In addition, the color of the primary teeth was darker compared to the cream white color of normal primary teeth (Figure 1b–e).

The panoramic radiograph of the proband showed that there was almost no enamel coverage on the erupted and developing tooth buds of permanent teeth (Figure 1f) comparing to that from a healthy age- and gender-matched child (Figure 1g). Notably, enamel in the deciduous teeth was nearly invisible as well (Figure 1f).

The mother's teeth appeared to be highly polished, while some localized opaque and white spots were evident, especially in the cervical third of the buccal side of maxillary first molar (Figure 1h). Besides this, no other alterations in enamel hardness or thickness were found. For the proband's father, some irregular localized enamel defects—circumscribed enamel pits, arranged in horizontal lines in the cervical third of the crown—were shown in the enamel (Figure 1j). In addition, exogenous pigmentation was also present on most of his teeth (Figure 1j). His panoramic radiograph showed normal-looking tooth structures (Figure 1i). The typical feature between phenotype and genotype of this family was consistent with autosomal-recessive transmission of generalized hypoplastic AI (Chan et al., 2010; Ozdemir et al., 2005).

3.2 | Scanning electron microscopy observation

The enamel layer of the affected deciduous tooth revealed poorly formed enamel rods with extensive irregular, disorganized rough-superficial enamel layer (Figure 2a and b). The course of the enamel prisms was abnormal, or could not be distinguished at all. Irregularly shaped empty spaces were present. Borders of the enamel prisms were undulated and structural shapes of prisms irregular (Figure 2a and b) as compared to normal prisms of healthy enamel (Figure 2c and d).
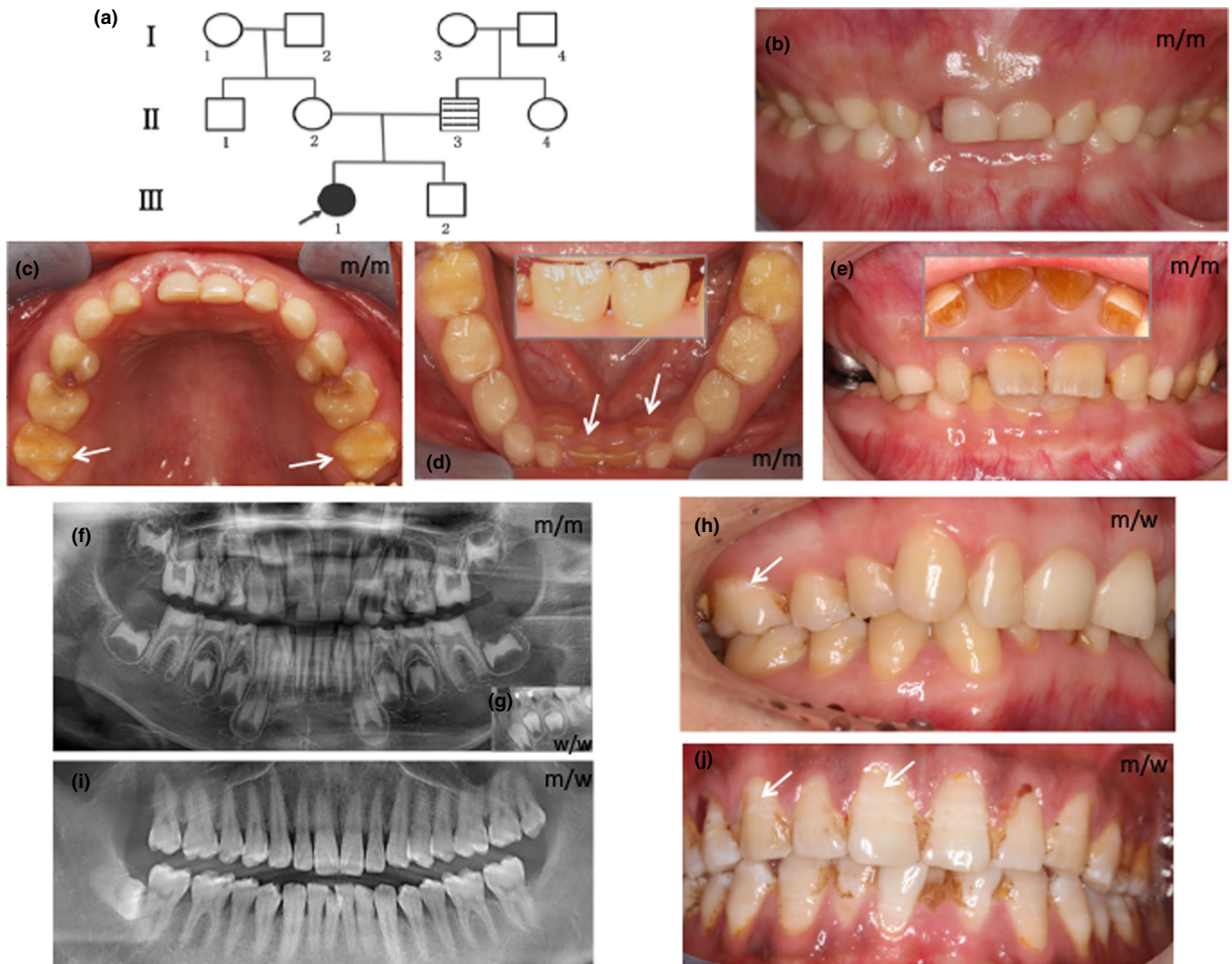
FIGURE 1 Pedigree and clinical phenotype. (a) Pedigree of the family: Males are marked as squares and females as circles. Filled symbols designate affected individuals; open symbols indicate those not affected; Horizontal strip lines symbol indicates localized enamel pitting. The black arrow is the proband. (b–e) Intraoral photographs of the proband (III: 1) at age 8 (b–d) and age 8 years and 9 months (e). The first molars and the mandible incisors were small, thin, and yellow due to the lack of enamel thickness (white arrows). Insert photograph showed the labial side of the mandible (d) and lingual side of maxillary incisors (e) separately. (f) Panoramic radiograph of the proband. (g) Insert box shows the density of normal teeth matched by age and gender. (h) Clinical photo of the proband's mother (II: 2). White arrow showed localized white spot in the enamel. (i) Panoramic radiograph of the proband's father. (j) Frontal clinical photo of the father (II: 3). White arrows showed irregular localized enamel defects. m/m, m/w, and w/w indicate homozygous mutant, heterozygous mutant and wild type, respectively

3.3 | A novel *ENAM* mutation identified by WES and variation screening

WES was performed for the proband in order to identify the potential causative genes. 15.60 Gb data of exome sequences were obtained on average and the mean sequencing depth was 106.32-fold. In total, 95.87% of the exonic regions were covered at least 20-fold, indicating high sequencing quality. The sequences were then mapped to the human GRCh37/hg19 reference genome and 83,924 single nucleotide variants and indels were identified. The above information indicated that both the quality and quantity of the sequencing data are suitable for further analysis.

Overall, among the known AI-causing genes, only a novel homozygous C-to-G mutation was identified in *ENAM* gene (c.2078C>G, p.(Ser693*)).

3.4 | Verification of the *ENAM* mutation by Sanger sequencing

The identified *ENAM* mutation (c.2078C>G, p.(Ser693*)) was verified subsequently by Sanger sequencing. The result showed that this mutation was unable to be detected in normal control (Figure 3a), while was identified in homozygous form in the proband (Figure 3b).
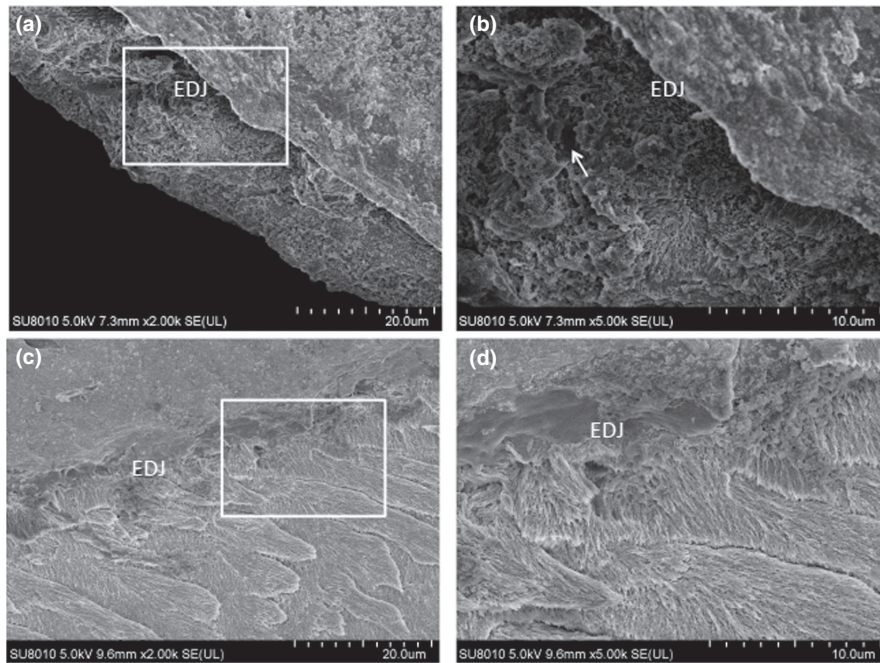
FIGURE 2 Ultrastructural phenotyping of affected enamel in deciduous tooth with the nonsense *ENAM* mutation (c.2078C>G; p.(Ser693*)). Scanning electron microscopy (SEM) of affected enamel (a, 1000×, b, 2000×) and the control (c, 1000×, d, 2000×) in deciduous teeth. The enamel layer of the affected deciduous tooth revealed poorly formed enamel rods with extensive irregular, disorganized rough superficial enamel layer. White arrow showed the irregularly shaped empty spaces
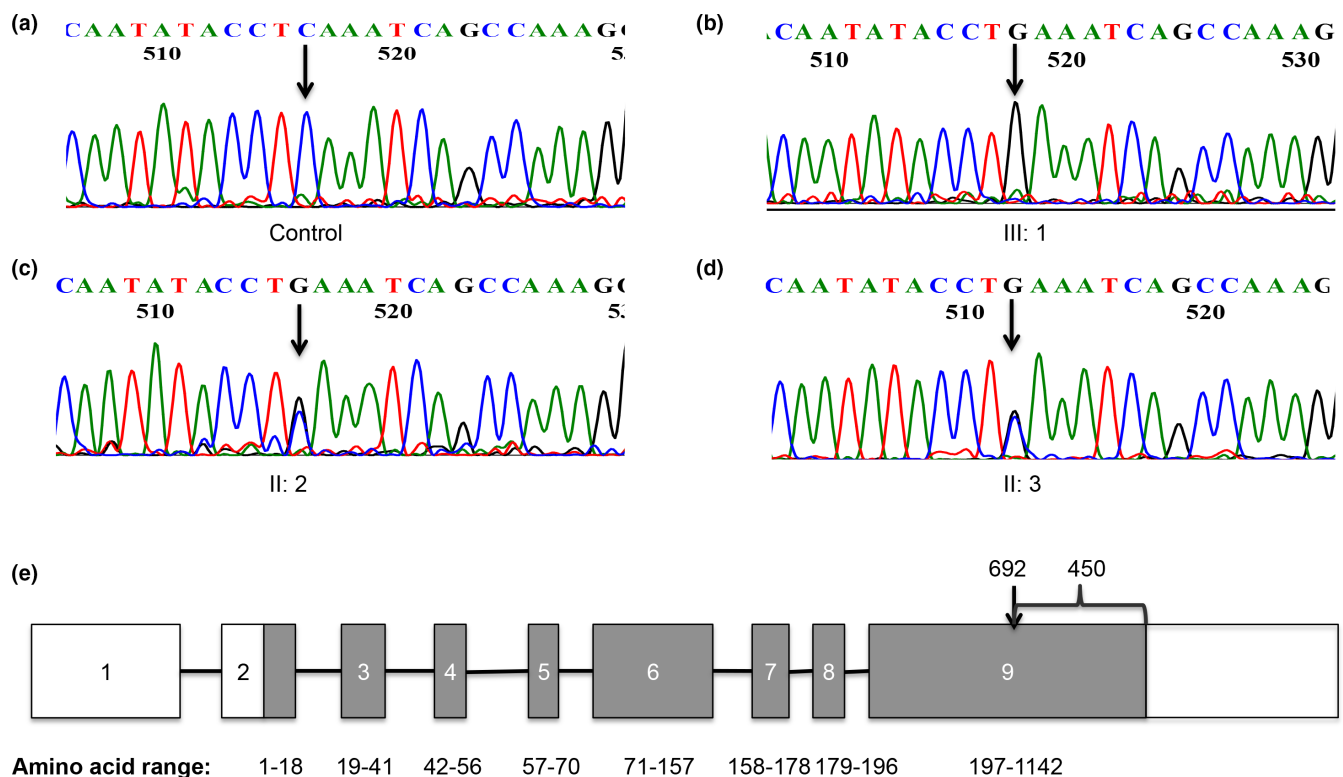

FIGURE 3 Verification of the identified mutation by Sanger sequencing. (a) A normal control DNA sequence of *ENAM* gene. (b) A homozygous *ENAM* mutation (c.2078C>G; p.(Ser693*)) identified in the proband. (c) A heterozygous mutation identified in the proband's mother. (d) A heterozygous mutation also identified in the proband's father. Both mutated and wild-type nucleotide residues are indicated by black arrows. (e) Schematic presentation of the structure of the *ENAM* gene containing the annotated mutation identified in this study. The exon coding regions are shaded. The black arrow indicates the position of the mutation

This mutation was also detected in proband's parents in heterozygous as expected (Figure 3 C and D), which was agreed with the autosomal-recessive inheritance pattern.

This mutation introduced a premature stop codon in the last exon of *ENAM* gene, which was predicted to result in a truncated peptide with 692 amino acids (Figure 3e). As the wild-type ENAM

was consisted of 1,142 amino acids, therefore, this mutation led to more than 30% loss of the full length of protein. The detected mutation has been submitted to GenBank (MT877227, http://www.ncbi.nlm.nih.gov/ genbank).

3.5 | Potential deleterious effects of the *ENAM* mutation

Three different in silico programs were used to predict the damaging effects of the detected nonsense mutation, such as CADD, M-CAP, and Mutation Taster. All the predicted results showed that the detected nonsense mutation (c.2078C>G, p.(Ser693*)) was deleterious and severely damaged the function of ENAM (Table 1).

In addition, the effect of the mutation on the 3D structure of ENAM protein was predicted by I-TASSER. The data, we presented here, were based on model 4 for the wild-type and the truncated proteins. There was an obvious difference between the 3D structure of mutated protein and that of wild type (Figure 4), leading to a loss of function of the predicted protein.

TABLE 1 Functional prediction of the *ENAM* variant

Prediction method	Score	Deleterious threshold	Misclassification rate
CADD-Phred	37	>20	26%
M-CAP	7.775	>0.025	5%
Mutation taster	1	>0.5	–

4 | DISCUSSION

In the study, a novel *ENAM* nonsense mutation (c.2078C>G, p.(Ser693*)) was identified in one Chinese family with hypoplastic AI in variable expressivity. The enamel of the proband with homozygous mutation was generalized hypoplastic. The clinical phenotype of the individuals harboring the heterozygous mutation varied from a lack of penetrance to mild enamel defects. Additional bioinformatics studies demonstrated that the detected mutation could change the 3D structure of the ENAM protein and impair the function of ENAM.

The human *ENAM* gene, encoding enamelin (ENAM), is localized on chromosome four and consists of nine exons and eight introns (Dong et al., 2000; Hu et al., 2000). As a tooth-specific protein, ENAM is expressed principally by ameloblasts in secretory stage (Hu & Yamakoshi, 2003). ENAM makes up 1 to 5% of the enamel matrix proteins (EMPs) and is the least in abundance of the three main enamel matrix proteins (Hu et al., 2000; Hu et al., 2001). In addition, ENAM plays a critical role for proper dental enamel formation. In vitro studies found that ENAM regulates the nucleation, growth, and organization of hydroxyapatite crystals (Hu et al., 2000; Hu et al., 2001). In *Enam*-null mice, the formation of enamel layer was interfered as a result of the lack of ENAM (Hu et al., 2008). Furthermore, disorganization and apoptosis of ameloblasts were also shown in *Enam*-null mice (Hu et al., 2011).

It was widely reported that defects in human *ENAM* gene could cause hypoplastic form AI, including autosomal-dominant and autosomal-recessive AI. The first reported mutation in *ENAM* resulted in AI was autosomal-dominant form and the patient showed a generalized thin hypoplastic phenotype (Rajpar et al., 2001). Autosomal-recessive inheritances were also documented for
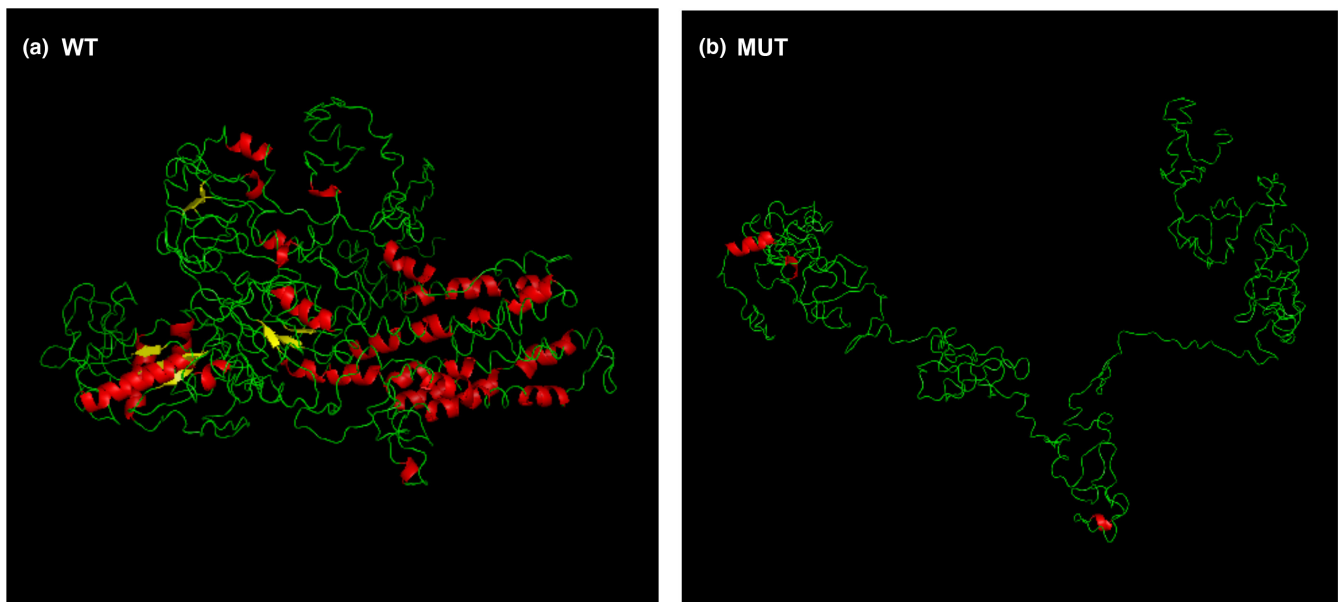

FIGURE 4 The 3D structure of ENAM predicted by I-TASSER in wild-type (a) and mutated ENAM (b). Helix (red), sheet (yellow), loop (green)

TABLE 2 Mutations described in *ENAM* to cause hypoplastic AI

No	cDNA	Protein	Type	Phenotypes and inheritance	References
1	c.92T>G	p.(Leu31Arg)	Missense	Generalized thin hypoplastic, AD	(Brookes et al., 2017)
2	c.107delA	p.(Asn36Ilefs*22)	Deletion	Local hypoplastic, AD	(Simmer et al., 2013)
3	c.123+1G>A	p.(Val19_Pro41del)	Splicing	AD	(Prasad et al., 2016)
4	c.123+2T>G	p.(Val19_Pro41del)	Splicing	Local hypoplastic, AD	(Koruyucu et al., 2018)
5	c.139delA	p.(Met47Cysfs*11)	Deletion	Local hypoplastic, AD	(Wang et al., 2015)
6	c.157A>T	p.(Lys53*)	Nonsense	Local hypoplastic, AD	(Kim et al., 2006; Mårdh et al., 2002)
7	c.211−2A>C	p.(Met71_Gln157del)	Splicing	Local hypoplastic, AD	(Kim et al., 2005)
8	c.358C>T	p.(Gln120*)	Nonsense	Local hypoplastic, AD	(Seymen et al., 2014)
9	c.395dupA	p.(Pro133Alafs*13)	Duplicate	Local hypoplastic, AD	(H. Zhang et al., 2019)
10	c.407_408insTCA AAAAAGCCGAC CACAA	p.(Lys136Asnfs*16)	Insertion	Local hypoplastic, AD	(Wang et al., 2015)
11	c.454G>T	p.(Glu152*)	Nonsense	Local hypoplastic, AD	(Seymen et al., 2014)
12	c.534+1G>A	p. Ala158_Gln178del	Splicing	Generalized thin hypoplastic, AD	(Rajpar et al., 2001)
13	c.535−2A>G	p.(Arg179_Gly196del)	Splicing	Generalized thin hypoplastic	(Wright et al., 2011)
14	c.536G>T	p.(Arg179Met)	Missense	Local hypoplastic, AD	(Gutierrez et al., 2007)
15	c.588+1delG	p.(Asn197Ilefs*81)	Deletion	Generalized thin hypoplastic or Localized, circumscribed pitting, AR/AD	(Dashash et al., 2011; P. S. Hart, Hart, et al., 2003; Kida et al., 2002; Kim et al., 2005; Pavlic et al.,2011; Wright et al., 2011; H. Zhang et al., 2019)
16	c.647C>T	p.(Ser216Leu)	Missense	Heterozygous carriers: Localized pitting, AD Compound heterozygotes: Generalized thin hypoplastic (c. 647C>T & c.1259_1260insAG), AR	(Chan et al., 2010)
17	c.737C>A	p.(Ser246*)	Nonsense	Local hypoplastic, AD	(Ozdemir et al., 2005)
18	c.1021_1022insGT CAGTACCAGTAC TGTGTCA	p.(Val340_Met341ins SerGlnTyrGlnTyrCysVal)	Insertion	Heterozygous carriers: Localized, circumscribed pitting, AD Compound heterozygotes: Generalized thin hypoplastic, (c.1020_I021insAGTCAGTACCAGTACTGTGTC & c.1259_1260insAG), AR	(Ozdemir et al., 2005)
19	c.1259_1260insAG	p.(Pro422Valfs*27)	Insertion	Generalized thin hypoplastic or Localized, circumscribed pitting, AR/AD	(Chan et al., 2010; T. C. Hart, Hart, et al., 2003; Kang et al., 2009; Lindemeyer et al.,2010; Ozdemir et al., 2005; Pavlic et al., 2007; Wright et al., 2011)
20	c.1842C>G	p.(Tyr614*)	Nonsense	Generalized thin hypoplastic, AR Heterozygous carriers: varied from a lack of penetrance to a local hypoplastic enamel defect, AR/AD	(Koruyucu et al., 2018)
21	c.2078C>G	p.(Ser693*)	Nonsense	Generalized thin hypoplastic, AR	This report
22	c.2763delT	p.(Asp921Glufs*32)	Deletion	Compound heterozygotes: c.1259_1260insAG & c.2763delT, AR	(H. Zhang et al., 2019)
23	c.2991delT	p.(Leu998Trpfs*65)	Deletion	Local hypoplastic, AD	(Kang et al., 2009)

ENAM mutations (Chan et al., 2010; Hart, Hart, et al., 2003; Ozdemir et al., 2005), in which heterozygotes usually presented with a milder, local form, while homozygotes showed a severe form (Ozdemir et al., 2005). At present, more than 20 different *ENAM* mutations were reported in AI with multiple mutation types, including missense, nonsense, splicing, duplicate, and insertion or deletion-caused frame-shift mutation (Table 2). The severe type of AI in homozygotes was often caused by frame-shift or nonsense mutations (Wang et al., 2015) thus producing a truncated protein (Miller & Pearce, 2014). It was also reported that same *ENAM* mutation might lead to phenotypic variations among different families (Hart, Michalec, et al., 2003).

The enamel phenotypes caused by *ENAM* mutations in humans show a clear dose-effect and variable expressivity. In present study, the proband had a homozygous *ENAM* mutation, causing severe generalized enamel malformations with almost no enamel covering dentin. Meanwhile, the proband's father who was heterozygous for one mutant allele, displayed localized enamel defects—circumscribed enamel pits, arranged in horizontal lines in the cervical third of the crown, which have been reported by others (Hart, Hart, et al., 2003; Kang et al., 2009). This very mild phenotype, which would not be traditionally diagnosed as AI, presents a challenge to the current AI nomenclature. Surprisingly, any abnormality was not found in enamel of the proband's mother except for some localized opaque and white spots in the cervical third of the maxillary first molar, although the heterozygous *ENAM* mutation was also present. Variable expressivity from localized hypoplasia to generalized severe enamel loss has been reported with c.588+1delG mutational hotspot in *ENAM*, p. (Asn197Ilefs*81), among different families and family members (Hart, Hart, et al., 2003; Kida et al., 2002; Kim et al., 2005; Pavlic et al., 2007). They all found that when a single *ENAM* allele was defective, the enamel malformations varied in severity and could be nonpenetrant, which was consistent with present study. Furthermore, the novel *ENAM* nonsense mutation (c.2078C>G, p.(Ser693*)) we identified introduced a premature stop codon which was in the last exon of *ENAM* gene. It is predicted that the mutant mRNA transcript would escape Nonsense-mediated Decay and be translated into a truncated ENAM protein (Miller & Pearce, 2014).

SEM was used to observe the ultrastructure alterations in AI. We found that the enamel layer of the affected primary teeth showed poorly formed enamel rods with extensive irregular, disorganized rough superficial enamel layer. The ultrastructure alteration of the permanent teeth was unable to be carried out due to the difficulty of collection of specimen. While similar phenotype of the primary teeth and permanent teeth of the proband were shown from the intraoral photographs with enamel markedly reduced in thickness, although the enamel in primary teeth looks thicker than permanent teeth. Therefore, similar ultrastructure alterations of the permanent teeth were speculated. The findings of present study were in agreement with previous reports on *ENAM* mutations (g.8344delG and g.13185–13186insAG), in which affected enamel is markedly reduced in thickness, lacks a normal prismatic structure and has a laminated appearance (Hart, Michalec, et al., 2003; Pavlic et al., 2007). While it is difficult to find the relationship between the ultrastructure alternations of affected enamel and the specific mutations, but these results could provide a new viewpoint for exploring the various harmful influences of *ENAM* mutations on different stages of enamel formation.

Mouse model study on ENAM also indicated that the quantity of ENAM played an essential role on normal enamel formation (Hu et al., 2014). However, for the extremely mild clinical phenotype or the lack of penetrance in certain individuals, there is still lack of study on direct mechanism. Inherited enamel malformations are highly heterogeneous. Further genetic and functional investigations are needed to understand the biological mechanism of enamel formation.

In summary, a novel *ENAM* nonsense mutation (c.2078C>G, p.(Ser693*)) was identified in one Chinese family with generalized hypoplastic AI. This nonsense mutation in *ENAM* gene resulted in a truncated protein and changed the 3D structure of ENAM. Our finding indicates that this mutation leads to the hypoplastic AI in present patient, which broaden the spectrum of known *ENAM* mutations in hypoplastic AI patients and provides evidence that *ENAM* mutations frequently exhibit wide variable expressivity and sometimes lack of penetrance. Insights into the association between the severe phenotypes and their mutations in hypoplastic AI patients also enhance our understandings of the cellular and molecular mechanisms involved in tooth enamel development.

CONFLICT OF INTERESTS

The authors declare that there are no conflicts of interest.

AUTHOR CONTRIBUTIONS

Shunlan Yu: Conceptualization; Data curation; Formal analysis; Funding acquisition; Investigation; Methodology; Project administration; Resources; Software; Validation; Visualization; Writing–original draft; Writing–review and editing. **Chenying Zhang:** Conceptualization; Data curation; Formal analysis; Investigation; Methodology; Project administration; Supervision; Validation; Visualization; Writing–review and editing. **Ce Zhu:** Data curation; Validation; Visualization; Writing-review & editing. **Dandan Liu:** Conceptualization; Methodology; Project administration. **Junkang Quan:** Project administration. **Xiaozhe Wang:** Data curation; Funding acquisition; Investigation; Project administration; Resources; Supervision; Validation; Writing–review and editing. **Shuguo Zheng:** Funding acquisition; Project administration; Supervision; Visualization.

PEER REVIEW

The peer review history for this article is available at https://publons.com/publon/10.1111/odi.13877.

REFERENCES

Bäckman, B., & Holm, A. K. (1986). Amelogenesis imperfecta: Prevalence and incidence in a northern Swedish county. *Community Dentistry and Oral Epidemiology*, *14*(1), 43–47. https://doi.org/10.1111/j.1600-0528.1986.tb01493.x

Brookes, S. J., Barron, M. J., Smith, C. E. L., Poulter, J. A., Mighell, A. J., Inglehearn, C. F., Brown, C. J., Rodd, H., Kirkham, J., & Dixon, M. J. (2017). Amelogenesis imperfecta caused by N-terminal enamelin point mutations in mice and men is driven by endoplasmic reticulum stress. *Human Molecular Genetics*, *26*(10), 1863–1876. https://doi.org/10.1093/hmg/ddx090

Chan, H.-C., Mai, L., Oikonomopoulou, A., Chan, H. L., Richardson, A. S., Wang, S.-K., Simmer, J. P., & Hu, J.-C. (2010). Altered enamelin phosphorylation site causes amelogenesis imperfecta. *Journal of Dental Research*, *89*(7), 695–699. https://doi.org/10.1177/0022034510365662

Dashash, M., Bazrafshani, M. R., Poulton, K., Jaber, S., Naeem, E., & Blinkhorn, A. S. (2011). Enamelin/ameloblastin gene polymorphisms in autosomal amelogenesis imperfecta among Syrian families. *Journal of Investigative and Clinical Dentistry*, *2*(1), 16–22. https://doi.org/10.1111/j.2041-1626.2010.00038.x

Dong, J., Gu, T. T., Simmons, D., & MacDougall, M. (2000). Enamelin maps to human chromosome 4q21 within the autosomal dominant amelogenesis imperfecta locus. *European Journal of Oral Sciences*, *108*(5), 353–358. https://doi.org/10.1034/j.1600-0722.2000.108005353.x

Gadhia, K., McDonald, S., Arkutu, N., & Malik, K. (2012). Amelogenesis imperfecta: An introduction. *British Dental Journal*, *212*(8), 377–379. https://doi.org/10.1038/sj.bdj.2012.314

Gutierrez, S. J., Chaves, M., Torres, D. M., & Briceno, I. (2007). Identification of a novel mutation in the enamalin gene in a family with autosomal-dominant amelogenesis imperfecta. *Archives of Oral Biology*, *52*(5), 503–506. https://doi.org/10.1016/j.archoralbio.2006.09.014

Hart, P. S., Michalec, M. D., Seow, W. K., Hart, T. C., & Wright, J. T. (2003). Identification of the enamelin (g.8344delG) mutation in a new kindred and presentation of a standardized ENAM nomenclature. *Archives of Oral Biology*, *48*(8), 589–596. https://doi.org/10.1016/s0003-9969(03)00114-6

Hart, T. C., Hart, P. S., Gorry, M. C., Michalec, M. D., Ryu, O. H., Uygur, C., & Firatli, E. (2003). Novel ENAM mutation responsible for autosomal recessive amelogenesis imperfecta and localised enamel defects. *Journal of Medical Genetics*, *40*(12), 900–906. https://doi.org/10.1136/jmg.40.12.900

Hintzsche, J. D., Robinson, W. A., & Tan, A. C. (2016). A survey of computational tools to analyze and interpret whole exome sequencing data. *International Journal of Genomics*, *2016*, 7983236. https://doi.org/10.1155/2016/7983236

Hu, C.-C., Hart, T. C., Dupont, B. R., Chen, J. J., Sun, X., Qian, Q., Zhang, C. H., Jiang, H., Mattern, V. L., Wright, J. T., & Simmer, J. P. (2000). Cloning human enamelin cDNA, chromosomal localization, and analysis of expression during tooth development. *Journal of Dental Research*, *79*(4), 912–919. https://doi.org/10.1177/00220345000790040501

Hu, J.-C., Hu, Y., Lu, Y., Smith, C. E., Lertlam, R., Wright, J. T., Suggs, C., McKee, M. D., Beniash, E., Kabir, M. E., & Simmer, J. P. (2014). Enamelin is critical for ameloblast integrity and enamel ultrastructure formation. *PLoS ONE*, *9*(3), e89303. https://doi.org/10.1371/journal.pone.0089303

Hu, J.-C., Hu, Y., Smith, C. E., McKee, M. D., Wright, J. T., Yamakoshi, Y., Papagerakis, P., Hunter, G. K., Feng, J. Q., Yamakoshi, F., & Simmer, J. P. (2008). Enamel defects and ameloblast-specific expression in Enam knock-out/lacz knock-in mice. *Journal of Biological Chemistry*, *283*(16), 10858–10871. https://doi.org/10.1074/jbc.M710565200

Hu, J. C., Lertlam, R., Richardson, A. S., Smith, C. E., McKee, M. D., & Simmer, J. P. (2011). Cell proliferation and apoptosis in enamelin null mice. *European Journal of Oral Sciences*, *119 Suppl 1*(Suppl 1), 329–337. https://doi.org/10.1111/j.1600-0722.2011.00860.x

Hu, J. C., & Yamakoshi, Y. (2003). Enamelin and autosomal-dominant amelogenesis imperfecta. *Critical Reviews in Oral Biology and Medicine*, *14*(6), 387–398.

Hu, J. C., Zhang, C. H., Yang, Y., Kärrman-Mårdh, C., Forsman-Semb, K., & Simmer, J. P. (2001). Cloning and characterization of the mouse and human enamelin genes. *Journal of Dental Research*, *80*(3), 898–902. https://doi.org/10.1177/00220345010800031001

Jagadeesh, K. A., Wenger, A. M., Berger, M. J., Guturu, H., Stenson, P. D., Cooper, D. N., Bernstein, J. A., & Bejerano, G. (2016). M-CAP eliminates a majority of variants of uncertain significance in clinical exomes at high sensitivity. *Nature Genetics*, *48*(12), 1581–1586. https://doi.org/10.1038/ng.3703

Kang, H. Y., Seymen, F., Lee, S. K., Yildirim, M., Tuna, E. B., Patir, A., & Kim, J. W. (2009). Candidate gene strategy reveals ENAM mutations. *Journal of Dental Research*, *88*(3), 266–269. https://doi.org/10.1177/0022034509333180

Kida, M., Ariga, T., Shirakawa, T., Oguchi, H., & Sakiyama, Y. (2002). Autosomal-dominant hypoplastic form of amelogenesis imperfecta caused by an enamelin gene mutation at the exon-intron boundary. *Journal of Dental Research*, *81*(11), 738–742. https://doi.org/10.1177/0810738

Kim, J. W., Seymen, F., Lin, B. P., Kiziltan, B., Gencay, K., Simmer, J. P., & Hu, J. C. (2005). ENAM mutations in autosomal-dominant amelogenesis imperfecta. *Journal of Dental Research*, *84*(3), 278–282. https://doi.org/10.1177/154405910508400314

Kim, J. W., Simmer, J. P., Lin, B. P., Seymen, F., Bartlett, J. D., & Hu, J. C. (2006). Mutational analysis of candidate genes in 24 amelogenesis imperfecta families. *Eur J Oral Sci*, *114*(Suppl 1), 3–12. https://doi.org/10.1111/j.1600-0722.2006.00278.x

Kim, J. W., Zhang, H., Seymen, F., Koruyucu, M., Hu, Y., Kang, J., & Hu, J. C. (2019). Mutations in RELT cause autosomal recessive amelogenesis imperfecta. *Clinical Genetics*, *95*(3), 375–383. https://doi.org/10.1111/cge.13487

Kircher, M., Witten, D. M., Jain, P., O'Roak, B. J., Cooper, G. M., & Shendure, J. (2014). A general framework for estimating the relative pathogenicity of human genetic variants. *Nature Genetics*, *46*(3), 310–315. https://doi.org/10.1038/ng.2892

Koruyucu, M., Kang, J., Kim, Y. J., Seymen, F., Kasimoglu, Y., Lee, Z. H., & Kim, J. W. (2018). Hypoplastic AI with highly variable expressivity caused by ENAM mutations. *Journal of Dental Research*, *97*(9), 1064–1069. https://doi.org/10.1177/0022034518763152

Lagerström, M., Dahl, N., Nakahori, Y., Nakagome, Y., Bäckman, B., Landegren, U., & Pettersson, U. (1991). A deletion in the amelogenin gene (AMG) causes X-linked amelogenesis imperfecta (AIH1). *Genomics*, *10*(4), 971–975. https://doi.org/10.1016/0888-7543(91)90187-j

Li, H., & Durbin, R. (2009). Fast and accurate short read alignment with Burrows-Wheeler transform. *Bioinformatics*, *25*(14), 1754–1760. https://doi.org/10.1093/bioinformatics/btp324

Lindemeyer, R. G., Gibson, C. W., & Wright, T. J. (2010). Amelogenesis imperfecta due to a mutation of the enamelin gene: Clinical case with genotype-phenotype correlations. *Pediatric Dentistry*, *32*(1), 56–60.

Mårdh, C. K., Bäckman, B., Holmgren, G., Hu, J. C., Simmer, J. P., & Forsman-Semb, K. (2002). A nonsense mutation in the enamelin gene causes local hypoplastic autosomal dominant amelogenesis imperfecta (AIH2). *Human Molecular Genetics*, *11*(9), 1069–1074. https://doi.org/10.1093/hmg/11.9.1069

McGrath, J. A., Gatalica, B., Li, K., Dunnill, M. G., McMillan, J. R., Christiano, A. M., & Uitto, J. (1996). Compound heterozygosity for a dominant glycine substitution and a recessive internal duplication mutation in the type XVII collagen gene results in junctional epidermolysis bullosa and abnormal dentition. *American Journal of Pathology*, *148*(6), 1787–1796.

Miller, J. N., & Pearce, D. A. (2014). Nonsense-mediated decay in genetic disease: Friend or foe? *Mutation Research*, *Reviews in Mutation Research*, *762*, 52–64. https://doi.org/10.1016/j.mrrev.2014.05.001

Ozdemir, D., Hart, P. S., Firatli, E., Aren, G., Ryu, O. H., & Hart, T. C. (2005). Phenotype of ENAM mutations is dosage-dependent. *Journal of Dental Research*, *84*(11), 1036–1041. https://doi.org/10.1177/154405910508401113

Paine, M. L., White, S. N., Luo, W., Fong, H., Sarikaya, M., & Snead, M. L. (2001). Regulated gene expression dictates enamel structure and tooth function. *Matrix Biology*, *20*(5–6), 273–292. https://doi.org/10.1016/s0945-053x(01)00153-6

Pavlic, A., Battelino, T., Trebusak Podkrajsek, K., & Ovsenik, M. (2011). Craniofacial characteristics and genotypes of amelogenesis imperfecta patients. *European Journal of Orthodontics*, *33*(3), 325–331. https://doi.org/10.1093/ejo/cjq089

Pavlic, A., Petelin, M., & Battelino, T. (2007). Phenotype and enamel ultrastructure characteristics in patients with ENAM gene mutations g.13185-13186insAG and 8344delG. *Archives of Oral Biology*, *52*(3), 209–217. https://doi.org/10.1016/j.archoralbio.2006.10.010

Plagnol, V., Curtis, J., Epstein, M., Mok, K. Y., Stebbings, E., Grigoriadou, S., Wood, N. W., Hambleton, S., Burns, S. O., Thrasher, A. J., Kumararatne, D., Doffinger, R., & Nejentsev, S. (2012). A robust model for read count data in exome sequencing experiments and implications for copy number variant calling. *Bioinformatics*, *28*(21), 2747–2754. https://doi.org/10.1093/bioinformatics/bts526

Poulter, J. A., El-Sayed, W., Shore, R. C., Kirkham, J., Inglehearn, C. F., & Mighell, A. J. (2014). Whole-exome sequencing, without prior linkage, identifies a mutation in LAMB3 as a cause of dominant hypoplastic amelogenesis imperfecta. *European Journal of Human Genetics*, *22*(1), 132–135. https://doi.org/10.1038/ejhg.2013.76

Poulter, J. A., Murillo, G., Brookes, S. J., Smith, C. E. L., Parry, D. A., Silva, S., Kirkham, J., Inglehearn, C. F., & Mighell, A. J. (2014). Deletion of ameloblastin exon 6 is associated with amelogenesis imperfecta. *Human Molecular Genetics*, *23*(20), 5317–5324. https://doi.org/10.1093/hmg/ddu247

Prasad, M. K., Geoffroy, V., Vicaire, S., Jost, B., Dumas, M., Le Gras, S., Switala, M., Gasse, B., Laugel-Haushalter, V., Paschaki, M., Leheup, B., Droz, D., Dalstein, A., Loing, A., Grollemund, B., Muller-Bolla, M., Lopez-Cazaux, S., Minoux, M., Jung, S., … Bloch-Zupan, A. (2016). A targeted next-generation sequencing assay for the molecular diagnosis of genetic disorders with orodental involvement. *Journal of Medical Genetics*, *53*(2), 98–110. https://doi.org/10.1136/jmedgenet-2015-103302

Rajpar, M. H., Harley, K., Laing, C., Davies, R. M., & Dixon, M. J. (2001). Mutation of the gene encoding the enamel-specific protein, enamelin, causes autosomal-dominant amelogenesis imperfecta. *Human Molecular Genetics*, *10*(16), 1673–1677. https://doi.org/10.1093/hmg/10.16.1673

Schwarz, J. M., Cooper, D. N., Schuelke, M., & Seelow, D. (2014). MutationTaster2: Mutation prediction for the deep-sequencing age. *Nature Methods*, *11*(4), 361–362. https://doi.org/10.1038/nmeth.2890

Seymen, F., Kim, Y. J., Lee, Y. J., Kang, J., Kim, T.-H., Choi, H., Koruyucu, M., Kasimoglu, Y., Tuna, E. B., Gencay, K., Shin, T. J., Hyun, H.-K., Kim, Y.-J., Lee, S.-H., Lee, Z. H., Zhang, H., Hu, J.-C., Simmer, J. P., Cho, E.-S., & Kim, J.-W. (2016). Recessive mutations in

ACPT, encoding testicular acid phosphatase, cause hypoplastic Amelogenesis Imperfecta. *American Journal of Human Genetics*, *99*(5), 1199–1205. https://doi.org/10.1016/j.ajhg.2016.09.018

Seymen, F., Lee, K. E., Koruyucu, M., Gencay, K., Bayram, M., Tuna, E. B., & Kim, J. W. (2014). ENAM mutations with incomplete penetrance. *Journal of Dental Research*, *93*(10), 988–992. https://doi.org/10.1177/0022034514548222

Simmer, S. G., Estrella, N. M., Milkovich, R. N., & Hu, J. C. (2013). Autosomal dominant amelogenesis imperfecta associated with ENAM frameshift mutation p.Asn36Ilefs56. *Clinical Genetics*, *83*(2), 195–197. https://doi.org/10.1111/j.1399-0004.2012.01887.x

Smith, C. E. L., Poulter, J. A., Antanaviciute, A., Kirkham, J., Brookes, S. J., Inglehearn, C. F., & Mighell, A. J. (2017). Amelogenesis Imperfecta; genes, proteins, and pathways. *Frontiers in Physiology*, *8*, 435. https://doi.org/10.3389/fphys.2017.00435

Smith, C. E. L., Whitehouse, L. L. E., Poulter, J. A., Wilkinson Hewitt, L., Nadat, F., Jackson, B. R., Manfield, I. W., Edwards, T. A., Rodd, H. D., Inglehearn, C. F., & Mighell, A. J. (2020). A missense variant in specificity protein 6 (SP6) is associated with amelogenesis imperfecta. *Human Molecular Genetics*, *29*(9), 1417–1425. https://doi.org/10.1093/hmg/ddaa041

Wang, X., Zhao, Y., Yang, Y., & Qin, M. (2015). Novel ENAM and LAMB3 mutations in Chinese families with hypoplastic amelogenesis imperfecta. *PLoS ONE*, *10*(3), e0116514. https://doi.org/10.1371/journal.pone.0116514

Witkop, C. J. Jr (1988). Amelogenesis imperfecta, dentinogenesis imperfecta and dentin dysplasia revisited: Problems in classification. *Journal of Oral Pathology*, *17*(9–10), 547–553. https://doi.org/10.1111/j.1600-0714.1988.tb01332.x

Wright, J. T., Torain, M., Long, K., Seow, K., Crawford, P., Aldred, M. J., Hart, P. S., & Hart, T. C. (2011). Amelogenesis imperfecta: Genotype-phenotype studies in 71 families. *Cells Tissues Organs*, *194*(2–4), 279–283. https://doi.org/10.1159/000324339

Yang, J., & Zhang, Y. (2015). I-TASSER server: New development for protein structure and function predictions. *Nucleic Acids Research*, *43*(W1), W174–181. https://doi.org/10.1093/nar/gkv342

Yuen, W. Y., Pasmooij, A. M., Stellingsma, C., & Jonkman, M. F. (2012). Enamel defects in carriers of a novel LAMA3 mutation underlying epidermolysis bullosa. *Acta Dermato Venereologica*, *92*(6), 695–696. https://doi.org/10.2340/00015555-1341

Zhang, H., Hu, Y., Seymen, F., Koruyucu, M., Kasimoglu, Y., Wang, S. K., & Hu, J. C. (2019). ENAM mutations and digenic inheritance. *Molecular genetics and genomic medicine*, *7*(10), e00928. https://doi.org/10.1002/mgg3.928

Zhang, X., Liu, Y., Wang, X., Sun, X., Zhang, C., & Zheng, S. (2017). Analysis of novel RUNX2 mutations in Chinese patients with cleidocranial dysplasia. *PLoS ONE*, *12*(7), e0181653. https://doi.org/10.1371/journal.pone.0181653

SUPPORTING INFORMATION

Additional supporting information may be found online in the Supporting Information section.

How to cite this article: Yu S, Zhang C, Zhu C, et al. A novel *ENAM* mutation causes hypoplastic amelogenesis imperfecta. *Oral Dis*. 2022;28:1610–1619. https://doi.org/10.1111/odi.13877